ARMY RESEARCH LABORATORY

A New Model for Turbulence Spectra and Correlations Based on Meijer's *G*-Functions

by D. Keith Wilson

ARL-TN-104

February 1998

Army Research Laboratory
Adelphi, MD 20783-1197

ARL-TN-104 **February 1998**

A New Model for Turbulence Spectra and Correlations Based on Meijer's *G*-Functions

D. Keith Wilson
Information Science and Technology Directorate, ARL

Abstract

A three-parameter model for turbulence spectra and correlation functions, based on Meijer's G-functions, is introduced. The model is more flexible than the traditional von Kármán model, but still allows the spectra and correlation functions to be derived analytically. The G-function model reduces to the von Kármán model for certain combinations of the parameters.

Contents

Figures

Tables

1. Introduction

One-half century ago, von Kármán (1948) suggested an equation to describe the spectrum of turbulence. This equation and various associated ones continue to be used widely. The main benefits of von Kármán's spectral equation are

1. A realistic inertial subrange: the spectra obey Kolmogorov's $-5/3$ power law (Kolmogorov, 1941) for wavenumbers k much larger than $1/L$, where L is a length scale characteristic of the larger eddies.
2. A realistic spectral rolloff in the energy subrange ($kL \ll 1$).
3. Analytical results can be derived for all spectral and correlation functions of interest.

In this note, I refer to von Kármán's equation and the various other spectra and correlations derived from it as "von Kármán's model." The von Kármán model appears in the literature in many different forms, but generally has two adjustable parameters. For the form used in this note, the parameters are a variance and a length scale. The variance parameter is set equal to the variance of the actual field. The length scale parameter is then chosen to reproduce the correct dissipation rate for the turbulence, which causes the model to agree with inertial-subrange data.

One drawback with the von Kármán model, with parameters chosen in this manner, is that it may not accurately describe the turbulence spectrum in the energy subrange. It appears typical that the predicted spectral levels for the energy subrange are less than actual data. Hence, it may be worthwhile in some applications to devise a new spectral model, similar to the von Kármán model, but allowing for more flexibility in fitting the energy-subrange region of the spectrum.

The purpose of this technical note is to propose such a model. The proposed model is based on manipulations of the general transcendental function known as the Meijer's G-function. It reduces to the von Kármán model as a special case.

2. Theory

2.1 One-Dimensional Spectra

The von Kármán equation for the longitudinal spectral density (i.e., the spectral density for velocity fluctuations with the wavenumber axis aligned with the velocity components) can be written in the form

$$\widehat{f}(k) = \frac{\sigma^2 \ell}{B(1/2, 1/3)} \frac{1}{(1 + k^2 \ell^2)^{5/6}}, \tag{1}$$

where σ^2 is the variance, ℓ a length scale, k the wavenumber (equal to 2π divided by the wavelength), and $B()$ the beta function. It can be easily verified that this equation obeys Kolmogorov's $k^{-5/3}$ power law in the inertial subrange ($k\ell \gg 1$).

A useful general property of longitudinal spectra is that the integral length scale is given by the equation (see, for example, Wilson, 1998)

$$L = \frac{\pi}{\sigma^2} \widehat{f}(0). \tag{2}$$

Hence for the von Kármán spectrum

$$L = \frac{\pi}{B(1/2, 1/3)} \ell, \tag{3}$$

and so we can also write the von Kármán spectrum in the alternative form

$$\widehat{f}(k) = \frac{\sigma^2 L}{\pi} \frac{1}{\left\{1 + [kLB(1/2, 1/3)/\pi]^2\right\}^{5/6}}. \tag{4}$$

The von Kármán spectrum agrees reasonably well with data from a variety of turbulence conditions. Generally, the main discrepancies are that the spectral peak (occurring at $k\ell \simeq 1$) is too sharp, and the predicted spectral levels in the energy subrange ($k\ell \ll 1$) are too low. Sometimes we desire a spectrum that describes these features of a dataset more realistically than the von Kármán spectrum. Kristensen et al. (1989) have suggested the following equation, which is very similar to the von Kármán spectrum:

$$\widehat{f}(k) = \frac{\sigma^2 L}{\pi} \frac{1}{\left\{1 + [kL/a(\mu)]^{2\mu}\right\}^{5/6\mu}}, \tag{5}$$

where

$$a(\mu) = \frac{\pi \mu}{B(1/2\mu, 1/3\mu)}. \tag{6}$$

The parameter μ affects the sharpness of the spectral peak. When $\mu = 1$, the Kristensen et al. spectrum reduces to the von Kármán spectrum. Kristensen et al. found that data for the neutral atmospheric shear layer were fit best using values of $\mu \simeq 0.5$. Hence, the actual turbulence spectra are less peaked than in the von Kármán model.

One drawback of Kristensen et al.'s spectrum is that the correlation function, which is the Fourier transform of the spectrum, cannot be determined analytically. Therefore, it would seem worthwhile to find spectral equations that behave similarly to Kristensen et al.'s, but can still be Fourier transformed. One possibility is

$$\widehat{f}(k) = \frac{\sigma^2 \ell}{3B(1/2, 1/3+b)} \left(k^2\ell^2\right)^{-5/6} B_{k^2\ell^2/(1+k^2\ell^2)}(5/6, b), \tag{7}$$

where $B_x(a, b)$ is the incomplete beta function. Using the fact that $B_x(a, 1) = x^a/a$, it can be shown that equation (7) reduces to the von Kármán spectrum when $b = 1$. Furthermore, since $B_x(a, b) \simeq x^a/a$ for $x \ll 1$,

$$\widehat{f}(0) = \frac{2\sigma^2 \ell}{5B(1/2, 1/3+b)}.$$

Hence, from equation (2),

$$L = \frac{2\pi}{5B(1/2, 1/3+b)} \ell. \tag{8}$$

Equation (7) can be written in two alternative forms involving higher transcendental functions, which will both be found useful later in this paper. Using equations (6.6.8) and (15.3.4) in Abramowitz and Stegun (1965), we find

$$\widehat{f}(k) = \frac{2\sigma^2 \ell}{5B(1/2, 1/3+b)} \, {}_2F_1\left(\frac{5}{6}, \frac{5}{6}+b; \frac{11}{6}; -k^2\ell^2\right), \tag{9}$$

where ${}_2F_1()$ is the hypergeometric function. Furthermore, using equations (5.6.1) and (5.3.8) in Erdélyi et al. (1953), we have

$$\widehat{f}(k) = \frac{\sigma^2 \ell}{3\Gamma(5/6+b) B(1/2, 1/3+b)} G_{22}^{12}\left(k^2\ell^2 \,\middle|\, \begin{matrix} 1/6, \ 1/6-b \\ 0, \ -5/6 \end{matrix}\right), \tag{10}$$

where $G_{pq}^{mn}()$ is the Meijer's G-function. The Meijer's G-function is a very general function, reducing to many of the more common functions, such as Bessel functions and hypergeometric functions as special cases. In the remainder of this paper, the turbulence model developed based on equation (7) (and, hence, also eq. (10)) will be called the *G-function model.*

2.2 Energy Spectrum

Assuming the flow is incompressible, and the turbulence homogeneous and isotropic, the energy spectrum can be found from the longitudinal spectrum using the equation (Batchelor, 1953)

$$E(k) = k^3 \frac{d}{dk}\left[\frac{1}{k}\frac{d\hat{f}(k)}{dk}\right]. \tag{11}$$

Although any of the forms for $\hat{f}(k)$ given by equations (7) to (10) can be substituted into the above, it is perhaps easiest to use equation (9) in conjunction with the differentiation formula for hypergeometric functions, Abramowitz and Stegun's (1965) equation (15.2.1). The result is

$$E(k) = \frac{8(5/6+b)(11/6+b)}{17B(1/2, 1/3+b)}\sigma^2 k^4 \ell^5 \, {}_2F_1\left(\frac{17}{6}, \frac{17}{6}+b; \frac{23}{6}; -k^2\ell^2\right). \tag{12}$$

Again using equations (6.6.8) and (15.3.4) in Abramowitz and Stegun (1965), the hypergeometric function can be rewritten in terms of the incomplete beta function:

$$E(k) = \frac{4(5/6+b)(11/6+b)}{3B(1/2, 1/3+b)}\sigma^2 \ell \left(k^2\ell^2\right)^{-5/6} B_{k^2\ell^2/(1+k^2\ell^2)}(17/6, b). \tag{13}$$

The form involving Meijer's G-functions is

$$E(k) = \frac{4\sigma^2\ell}{3\Gamma(5/6+b)\,B(1/2, 1/3+b)} G_{22}^{12}\left(k^2\ell^2 \,\middle|\, \begin{matrix} 1/6, \; 1/6-b \\ 2, \; -5/6 \end{matrix}\right). \tag{14}$$

Equations (5.6.74) and (5.3.8) in Erdélyi et al. (1953) were used to derive this result.

2.3 Longitudinal Correlation Function

The longitudinal correlation function $f(r)$ is the Fourier cosine transform of the longitudinal spectrum:

$$f(r) = 2\int_0^\infty \hat{f}(k)\cos(kr)\,dk. \tag{15}$$

The solution to this integral is known when the form of $\hat{f}(k)$ involving Meijer's G-functions (eq (10)) is used. Specifically, from equation (7.815.2) in Gradshteyn and Ryzhik (1994), we have

$$f(r) = \frac{2\sqrt{\pi}\sigma^2\ell}{3r\Gamma(5/6+b)\,B(1/2, 1/3+b)} G_{42}^{13}\left(\frac{4\ell^2}{r^2} \,\middle|\, \begin{matrix} 1/2, \; 1/6, \; 1/6-b, \; 0 \\ 0, \; -5/6 \end{matrix}\right).$$

This result can be reduced to lower order using equations (5.3.7) and (5.3.9) in Erdélyi et al. (1953). We obtain

$$f(r) = \frac{\sqrt{\pi}\sigma^2}{3\Gamma(5/6+b)\,B(1/2,1/3+b)}\left(\frac{r}{2\ell}\right) G_{13}^{30}\left(\frac{r^2}{4\ell^2}\middle|\begin{matrix}5/6\\ -1/2,\ -1/6,\ b-1/6\end{matrix}\right). \tag{16}$$

Apparently this result cannot be rewritten in terms of more common functions, such as modified Bessel functions or hypergeometric functions. When $b = 1$, though, the G-function can be reduced to one of lower order using equation (5.3.7) in Erdélyi et al., and we have

$$f(r) = \frac{\sigma^2}{\Gamma(1/3)}\left(\frac{r}{2\ell}\right) G_{02}^{20}\left(\frac{r^2}{4\ell^2}\middle| -1/2,\ -1/6\right). \tag{17}$$

The function G_{02}^{20} can be related to a modified Bessel function using equation (5.6.3) in Erdélyi et al., with the result

$$f(r) = \frac{2\sigma^2}{\Gamma(1/3)}\left(\frac{r}{2\ell}\right)^{1/3} K_{1/3}\left(\frac{r}{\ell}\right). \tag{18}$$

This is the correlation function for the von Kármán model.

2.4 Two-Dimensional Correlation Function

The two-dimensional (2D) correlation function is important for studies of wave propagation through turbulence. It can be determined from the energy spectrum using the equation (e.g., Wilson, 1998)

$$b(r) = \frac{1}{2}\int_0^\infty E(k) J_0(rk)\,\frac{dk}{k}. \tag{19}$$

When the energy spectrum in terms of hypergeometric functions (eq (12)) is substituted into equation (19), we can write the result of the integration in terms of Meijer's G-functions using equation (7.542.8) in Gradshteyn and Ryzhik (1994). Simplifying the result using equations (5.3.7) and (5.3.8) in Erdélyi et al. (1953), we find

$$\begin{aligned} b(r) &= \frac{\sigma^2\ell}{3\Gamma(5/6+b)\,B(1/2,1/3+b)}\left[G_{13}^{30}\left(\frac{r^2}{4\ell^2}\middle|\begin{matrix}11/6\\ 0,\ 5/6,\ b+5/6\end{matrix}\right)\right.\\ &\quad \left. - G_{13}^{30}\left(\frac{r^2}{4\ell^2}\middle|\begin{matrix}11/6\\ 1,\ 5/6,\ b+5/6\end{matrix}\right)\right]. \end{aligned} \tag{20}$$

As was the case for the longitudinal correlation function, the G-functions simplify to modified Bessel functions when $b = 1$. The result is

$$b(r) = \frac{2\sigma^2 \ell}{\sqrt{\pi}\Gamma(1/3)} \left(\frac{r}{2\ell}\right)^{5/6} \left[K_{5/6}\left(\frac{r}{\ell}\right) - \left(\frac{r}{2\ell}\right) K_{1/6}\left(\frac{r}{\ell}\right)\right]. \tag{21}$$

2.5 Parameter Selection

The von Kármán spectrum has two adjustable parameters: the variance σ^2 and the length scale ℓ. We can determine the variance parameter by setting it equal to the variance of a given data set. The length scale can be determined by matching the inertial subrange asymptote ($k\ell \gg 1$) of the data. The inertial-subrange asymptote in the von Kármán model is

$$\widehat{f}(k) \simeq \frac{\sigma^2 \ell^{-2/3}}{B(1/2, 1/3)} k^{-5/3}. \tag{22}$$

The Kolmogorov theory for the inertial subrange leads to the equation (Kaimal et al., 1972)

$$\widehat{f}(k) \simeq \frac{\alpha_1}{2} \epsilon^{2/3} k^{-5/3}, \tag{23}$$

where α_1 is a constant whose value is approximately 0.52, and ϵ is the dissipation rate of turbulent kinetic energy. Comparing equations (22) and (23), we see

$$\ell = \left[\frac{2}{\alpha_1 B(1/2, 1/3)}\right]^{3/2} \frac{\sigma^3}{\epsilon}. \tag{24}$$

When this relationship is used, our two underlying parameters for the von Kármán model become σ^2 and ϵ. The length scale parameter depends on the ratio σ^3/ϵ. From equation (3), the *predicted* value (not the *actual* value) of the integral length scale for the von Kármán model is

$$L_{vK} = \frac{\pi}{[B(1/2, 1/3)]^{5/2}} \left(\frac{2}{\alpha_1}\right)^{3/2} \frac{\sigma^3}{\epsilon}. \tag{25}$$

In the Kristensen et al. and G-function models, there is one additional adjustable parameter: μ for the former model, and b for the latter. We can adjust these parameters so that the actual value of the integral length scale of a given dataset, along with the variance and dissipation rates, are reproduced. The inertial-subrange asymptote for the Kristensen et al. model is

$$\widehat{f}(k) \simeq \frac{\sigma^2 L^{-2/3}}{\pi} \left[\frac{\pi\mu}{B(1/2\mu, 1/3\mu)}\right]^{5/3} k^{-5/3}. \tag{26}$$

Hence,

$$L = \pi \left[\frac{\mu}{B\left(1/2\mu, 1/3\mu\right)}\right]^{5/2} \left(\frac{2}{\alpha_1}\right)^{3/2} \frac{\sigma^3}{\epsilon}. \tag{27}$$

The ratio of the integral length scale to the value predicted by the von Kármán model is

$$\frac{L}{L_{vK}} = \left[\frac{\mu B\left(1/2, 1/3\right)}{B\left(1/2\mu, 1/3\mu\right)}\right]^{5/2}. \tag{28}$$

The inertial-subrange asymptote for the G-function model can be determined using the approximation $B_x\left(a, b\right) \simeq B\left(a, b\right)$ for $x \to 1$. We find

$$\widehat{f}\left(k\right) \simeq \frac{\sigma^2 \ell^{-2/3}}{3B\left(5/6, b\right)} k^{-5/3}. \tag{29}$$

Hence,

$$\ell = \left[\frac{2B\left(5/6, b\right)}{3\alpha_1 B\left(1/2, 1/3 + b\right)}\right]^{3/2} \frac{\sigma^3}{\epsilon},$$

$$L = \frac{6\pi}{5} \left[\frac{1}{3B\left(1/2, 1/3 + b\right)}\right]^{5/2} \left[\frac{2B\left(5/6, b\right)}{\alpha_1}\right]^{3/2} \frac{\sigma^3}{\epsilon}, \tag{30}$$

and

$$\frac{L}{L_{vK}} = \left[\frac{5}{6} B\left(5/6, b\right)\right]^{3/2} \left[\frac{2B\left(1/2, 1/3\right)}{5B\left(1/2, 1/3 + b\right)}\right]^{5/2}. \tag{31}$$

Table 1 shows the values of b and μ needed to reproduce certain values of the ratio L/L_{vK}.

Curves showing the dependence of L/L_{vK} on the parameter b for the G-function model and the dependence on μ for the Kristensen et al. model, are given in figure 1.

Table 1. Values for b and μ needed to reproduce certain values of ratio L/L_{vK}.

L/L_{vK}	b	μ
1	1	1
2	0.222	0.544
3	0.137	0.442

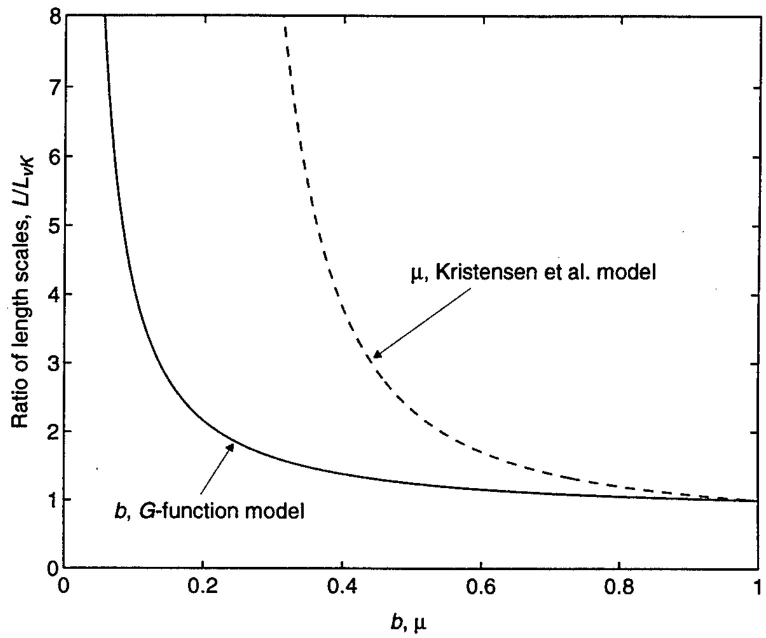

Figure 1. Dependence of ratio L/L_{vK} on parameter b for G-function model, and on μ for Kristensen et al. model.

3. Results and Discussion

The Meijer's G-functions in the proposed model can be calculated using the routines in the commercial software package Mathematica. I was unable to find such routines from any other source.

A comparison of the longitudinal spectra for the von Kármán, Kristensen et al., and G-function models is shown in figure 2. The same variance and dissipation rates were used in all three models. This results in the same inertial-subrange asymptote for all the models, as well as the same area under the curves. Two curves each are shown for the Kristensen et al. and G-function models, one with the integral length scale equal to twice the value in the von Kármán model, and the other three times the value in the von Kármán model. Note that when the integral length scale in either the Kristensen et al. or G-function model equals the value in the von Kármán model, the former models reduce to the von Kármán model. The Kristensen et al. and G-function models are observed to give similar predictions. However, there are two notable differences: the peak in the G-function model occurs at a lower wavenumber, and the transition from the peak to the inertial subrange is more gradual.

The energy spectrum for the G-function model is shown in figure 3. Curves for $L/L_{vK} = 1$, 2, and 3 are shown. ($L/L_{vK} = 1$ is the von Kármán model.) As with the one-dimensional spectra, increasing the ratio L/L_{vK} moves the peak wavelength to smaller values, while preserving the area under the curve.

Curves for the longitudinal correlation function of the G-function model are shown in figure 4. The main effect of increasing the integral length scale is to increase the area under the correlation curves.

The 2D correlation function for the G-function model is shown in figure 5. The 2D structure function, defined as

$$d(r) = 2\left[b(0) - b(r)\right], \tag{32}$$

is shown in figure 6. (The coherence of a propagating wave depends on the 2D structure function (Wilson, 1998).) Although the appearance of the curves in figure 6 suggests that the inertial subrange asymptote ($r/L_{vK} \ll 1$) in the G-function model depends on the ratio L/L_{vK}, in actuality the curves do converge for very small values of r/L_{vK}. Only when $r/L_{vK} \lesssim 10^{-8}$ do they differ by less than 1 percent. For large separations ($r/L_{vK} \gg 1$), increasing L/L_{vK} leads to larger values of the structure function.

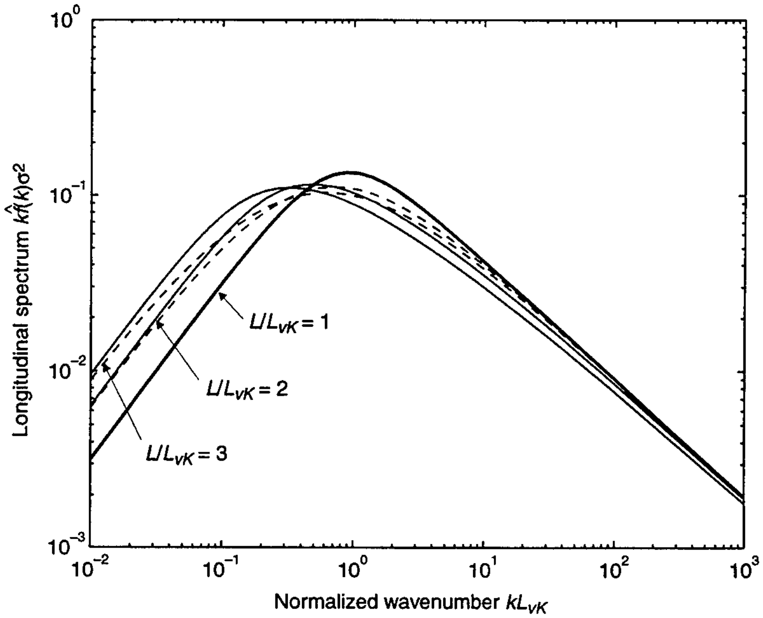

Figure 2. Longitudinal (one-dimensional) spectra for von Kármán, Kristensen et al., and G-function models. Kristensen et al. (dashed lines) and G-function (solid lines) models are shown for integral length scale L equal to twice and three times value in von Kármán model L_{vK}. Dark solid line is von Kármán model, and also Kristensen et al. and G-function models with $L/L_{vK} = 1$.

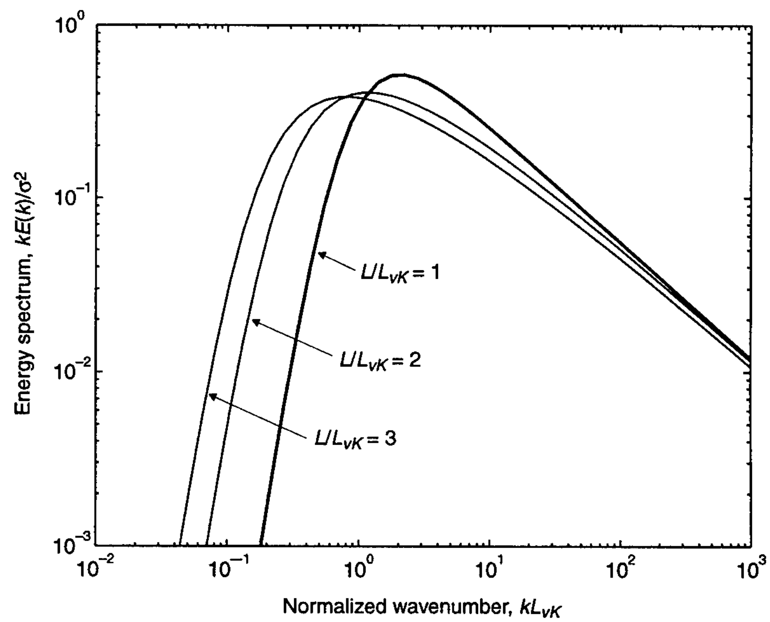

Figure 3. Energy spectrum of G-function model for several values of ratio L/L_{vK}.

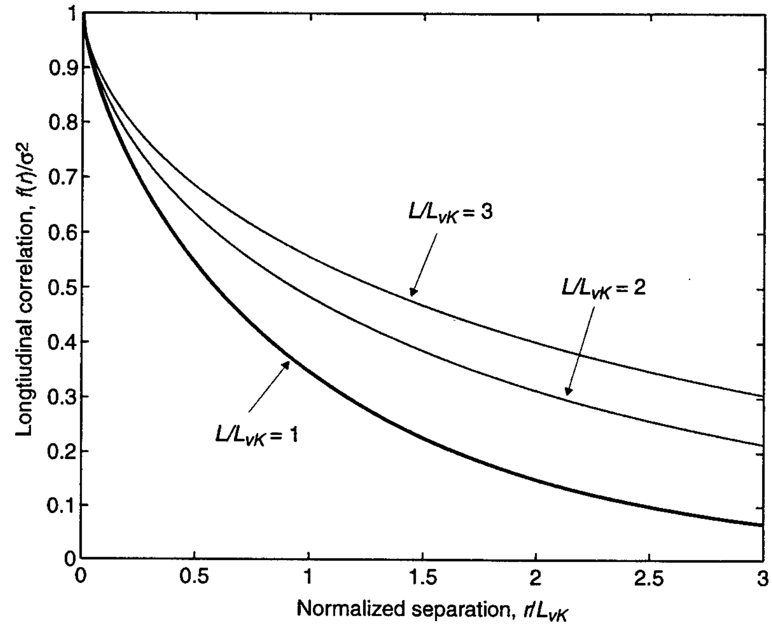

Figure 4. Longitudinal correlation function for G-function for several values of ratio L/L_{vK}.

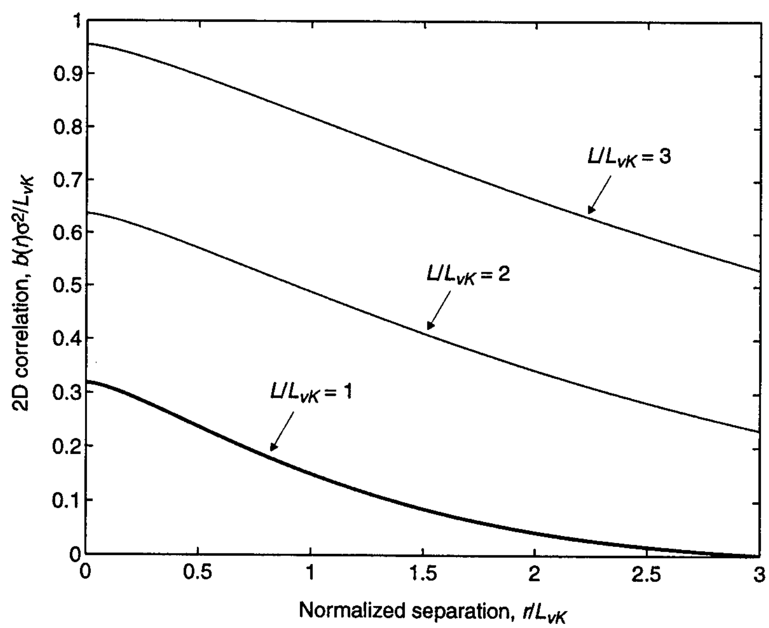

Figure 5. Two-dimensional correlation function for G-function model for several values of ratio L/L_{vK}.

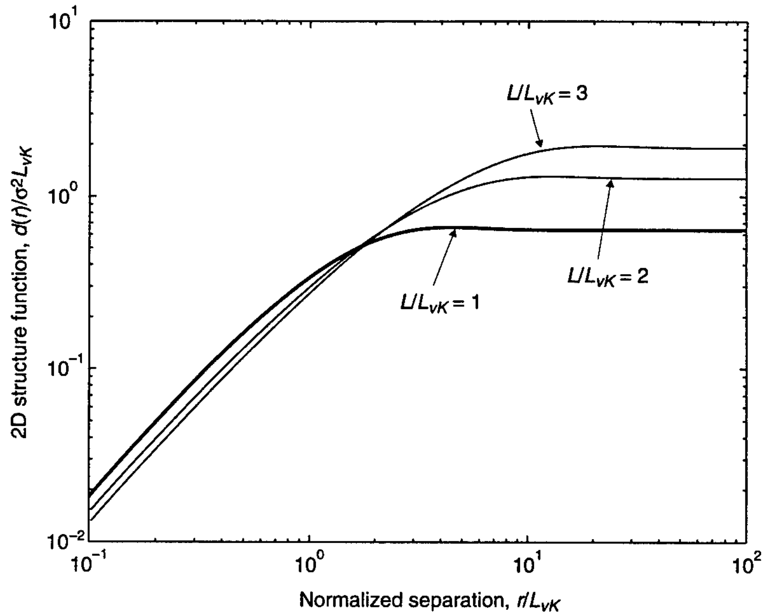

Figure 6. Two-dimensional structure function for G-function model for several values of ratio L/L_{vK}

4. Concluding Remarks

The G-function model is a reasonable generalization of the von Kármán model, offering the potential for improved accuracy in the modeling of turbulence spectra and correlation functions. Comparisons with experimental data, and more experience with application of the model, are needed to determine the model's true value.

It is possible to devise other three-parameter models based on Meijer's G-functions, besides the specific one proposed in this note. If agreement between data and the model proposed here is unsatisfactory, it may be worthwhile to attempt such alternative formulations.

One of the drawbacks of the G-function model is that routines to compute Meijer's G-functions are required to calculate the correlation functions. At the present time, only Mathematica offers this capability. However, it is likely that such routines will become more widely available during the coming decade.

Acknowledgement

Thanks to H. Auvermann of ARL for drawing my attention to the availability of Meijer's G-function routines in Mathematica.

References

Abramowitz, M., and I. A. Stegun, 1965: *Handbook of Mathematical Functions.* Dover, San Francisco, 675–679.

Batchelor, G. K., 1953: *The Theory of Homogeneous Turbulence.* Cambridge Univ. Press, Cambridge, Great Britain.

Erdélyi, A., W. Magnus, F. Oberhettinger, and F. G. Tricomi, 1953: *Higher Transcendental Functions,* volume 1. McGraw-Hill, New York.

Gradshteyn, I. S., and I. M. Ryzhik, 1994: *Table of Integrals, Series, and Products.* Academic Press, San Diego.

Kaimal, J. C., J. C. Wyngaard, Y. Izumi, and O. R. Coté, 1972: Spectral characteristics of surface layer turbulence. *Q. J. R. Meteorol. Soc.* **98**, 563–589.

Kolmogorov, A. N., 1941: The local structure of turbulence in incompressible viscous fluid for very large Reynolds numbers. *C. R. Acad. Sci. URSS* **30**, 301–305.

Kristensen, L., D. H. Lenschow, P. Kirkegaard, and M. Courtney, 1989: The spectral velocity tensor for homogeneous boundary-layer turbulence. *Bound. Layer Meteorol.* **47**, 149–193.

von Kármán, T., 1948: Progress in the statistical theory of turbulence. *Proc. National Acad. Sci.* **34**, 530–539.

Wilson, D. K., 1998: Anisotropic turbulence models for acoustic propagation through the neutral, atmospheric surface layer. U.S. Army Research Laboratory, ARL-TR-1519.

Distribution

Admnstr
Defns Techl Info Ctr
Attn DTIC-OCP
8725 John J Kingman Rd Ste 0944
FT Belvoir VA 22060-6218

Mil Asst for Env Sci Ofc of the Undersec of Defns for Rsrch & Engrg R&AT E LS
Pentagon Rm 3D129
Washington DC 20301-3080

Ofc of the Dir Rsrch and Engrg
Attn R Menz
Pentagon Rm 3E1089
Washington DC 20301-3080

Ofc of the Secy of Defns
Attn ODDRE (R&AT) G Singley
Attn ODDRE (R&AT) S Gontarek
The Pentagon
Washington DC 20301-3080

OSD
Attn OUSD(A&T)/ODDDR&E(R) J Lupo
Washington DC 20301-7100

ARL Chemical Biology Nuc Effects Div
Attn AMSRL-SL-CO
Aberdeen Proving Ground MD 21005-5423

Army Dugway Proving Ground
Attn STEDP 3
Attn STEDP-MT-DA-L-3
Attn STEDP-MT-M Bowers
Dugway UT 84022-5000

Army Missile Cmnd
Attn AMSMI-RD-AS-SS R Alongi
Redstone Arsenal AL 35898-5253

Army Rsrch Ofc
Attn AMXRO-GS Bach
PO Box 12211
Research Triangle Park NC 27709

Dir of Assessment and Eval
Attn SARD-ZD H K Fallin Jr
103 Army Pentagon Rm 2E673
Washington DC 20301-0163

Dpty Assist Secy for Rsrch & Techl
Attn SARD-TT F Milton Rm 3E479
The Pentagon
Washington DC 20301-0103

Hdqtrs Dept of the Army
Attn DAMO-FDT D Schmidt
400 Army Pentagon Rm 3C514
Washington DC 20301-0460

Natl Security Agency
Attn W21 Longbothum
9800 Savage Rd
FT George G Meade MD 20755-6000

US Army Avn Rsrch, Dev, & Engrg Ctr
Attn T L House
4300 Goodfellow Blvd
St Louis MO 63120-1798

US Army CECOM Rsrch, Dev, & Engrg
Attn R F Giordano
FT Monmouth NJ 07703-5201

US Army Edgewood Rsrch, Dev, & Engrg Ctr
Attn SCBRD-TD J Vervier
Aberdeen Proving Ground MD 21010-5423

US Army Matl Cmnd
Dpty CG for RDE Hdqtrs
Attn AMCRD BG Beauchamp
5001 Eisenhower Ave
Alexandria VA 22333-0001

US Army Matl Cmnd
Prin Dpty for Acquisition Hdqrts
Attn AMCDCG-A D Adams
5001 Eisenhower Ave
Alexandria VA 22333-0001

US Army Matl Cmnd
Prin Dpty for Techlgy Hdqrts
Attn AMCDCG-T M Fisette
5001 Eisenhower Ave
Alexandria VA 22333-0001

US Army Mis Cmnd (USAMICOM)
Attn AMSMI-RD-CS-R Documents
Redstone Arsenal AL 35898-5400

Distribution

US Army Nuclear & Chem Agency
Attn MONA-ZB
Bldg 2073
Springfield VA 22150-3198

US Army OEC
Attn CSTE-EFS
Park Center IV 4501 Ford Ave
Alexandria VA 22302-1458

US Army Rsrch Ofc
Attn G Iafrate
4300 S Miami Blvd
Research Triangle Park NC 27709

US Army Test & Eval Cmnd
Attn R G Pollard III
berdeen Proving Ground MD 21005-5055

US Army TRADOC Anlys Cmnd—WSMR
Attn ATRC-WSS-R
White Sands Missile Range NM 88002

US Army Train & Doctrine Cmnd
Battle Lab Integration & Techl Dirctrt
Attn ATCD-B J A Klevecz
FT Monroe VA 23651-5850

US Military Academy
Dept of Mathematical Sci
Attn MAJ D Engen
West Point NY 10996

USACRREL
Attn CEREL-GP R Detsch
72 Lyme Rd
Hanover NH 03755-1290

Nav Air War Cen Wpn Div
Attn CMD 420000D C0245 A Shlanta
1 Admin Cir
China Lake CA 93555-6001

Nav Surface Warfare Ctr
Attn Code B07 J Pennella
17320 Dahlgren Rd Bldg 1470 Rm 1101
Dahlgren VA 22448-5100

Naval Surface Weapons Ctr
Attn Code G63
Dahlgren VA 22448-5000

Air Weather Service
Attn TechL Lib FL4414 3
Scott AFB IL 62225-5458

Phillips Lab Atmospheric Sci Div
Geophysics Dirctrt
Hanscom AFB MA 01731-5000

Phillips Laboratory
Attn PL/LYP Chisholm
Hanscom AFB MA 01731-5000

DARPA
Attn B Kaspar
Attn L Stotts
3701 N Fairfax Dr
Arlington VA 22203-1714

Nasa Marshal Space Flt
Ctr Atmospheric Sciences Div
Attn E501 Fichtl
Huntsville AL 35802

Nasa Spct Flt Ctr
Atmospheric Sciences Div
Attn Code ED 41 1
Huntsville AL 35812

ARL Electromag Group
Attn Campus Mail Code F0250 A Tucker
University of Texas
Austin TX 78712

Univ of MississippiNCPA
Attn H E Bass
University MS 38577

Dept of Commerce Ctr
Mountain Administration
Attn Spprt Ctr Library R51
325 S Broadway
Boulder CO 80303

Natl Ctr for Atmospheric Research
Attn NCAR Library Serials
PO Box 3000
Boulder CO 80307-3000

Distribution

NCSU
Attn J Davis
PO Box 8208
Raleigh NC 27650-8208

US Army Rsrch Lab
Attn AMSRL-CI-LL Techl Lib (3 copies)
Attn AMSRL-CS-AL-TA Mail & Records Mgmt

US Army Rsrch Lab (cont'd)
Attn AMSRL-CS-AL-TP Techl Pub (3 copies)
Attn AMSRL-IS-E Battlefield Environ Div
Attn AMSRL-IS-EE D K Wilson (15 copies)
Attn AMSRL-SE-EE Z G Sztankay
Attn AMSRL-SE-SA N Srour
Adelphi MD 20783-1197

REPORT DOCUMENTATION PAGE

Form Approved OMB No. 0704-0188

1. AGENCY USE ONLY *(Leave blank)*	2. REPORT DATE	3. REPORT TYPE AND DATES COVERED
	February 1998	Final, November 1997 to January 1998

4. TITLE AND SUBTITLE

A New Model for Turbulence Spectra and Correlations Based on Meijer's *G*-Functions

5. FUNDING NUMBERS

DA Proj: B53A
PE: 61102A

6. AUTHOR(S)

D. Keith Wilson

7. PERFORMING ORGANIZATION NAME(S) AND ADDRESS(ES)

U.S. Army Research Laboratory
Attn: AMSRL-IS-EE (dkwilson@arl.mil)
2800 Powder Mill Road
Adelphi, MD 20783-1197

8. PERFORMING ORGANIZATION REPORT NUMBER

ARL-TN-104

9. SPONSORING/MONITORING AGENCY NAME(S) AND ADDRESS(ES)

U.S. Army Research Laboratory
2800 Powder Mill Road
Adelphi, MD 20783-1197

10. SPONSORING/MONITORING AGENCY REPORT NUMBER

11. SUPPLEMENTARY NOTES

AMS code: 61110253A11
ARL PR: 8FEJ60

12a. DISTRIBUTION/AVAILABILITY STATEMENT

Approved for public release; distribution unlimited.

12b. DISTRIBUTION CODE

13. ABSTRACT *(Maximum 200 words)*

A three-parameter model for turbulence spectra and correlation functions, based on Meijer's *G*-functions, is introduced. The model is more flexible than the traditional von Kármán model, but still allows the spectra and correlation functions to be derived analytically. The *G*-function model reduces to the von Kármán model for certain combinations of the parameters.

14. SUBJECT TERMS	15. NUMBER OF PAGES
Turbulence spectra, correlation functions, Meijer's *G*-function	27
	16. PRICE CODE

17. SECURITY CLASSIFICATION OF REPORT	18. SECURITY CLASSIFICATION OF THIS PAGE	19. SECURITY CLASSIFICATION OF ABSTRACT	20. LIMITATION OF ABSTRACT
Unclassified	Unclassified	Unclassified	UL

NSN 7540-01-280-5500

Standard Form 298 (Rev. 2-89)
Prescribed by ANSI Std. Z39-18
298-102